



# 1 **Inferring the effects of sink strength on plant carbon balance processes** 2 **from experimental measurements**

3 Kashif Mahmud<sup>1</sup>, Belinda E. Medlyn<sup>1</sup>, Remko A. Duursma<sup>1</sup>, Courtney Company<sup>1,2</sup>, Martin  
 4 G. De Kauwe<sup>3</sup>

5

6 <sup>1</sup>Hawkesbury Institute for the Environment, Western Sydney University, Locked Bag 1797,  
 7 Penrith NSW 2751, Australia

8 <sup>2</sup>Department of Biology, Colgate University, NY 13346, USA

9 <sup>3</sup>ARC Centre of Excellence for Climate Extremes, University of New South Wales, Sydney,  
 10 NSW 2052, Australia

11 *Correspondence to:* Kashif Mahmud ([k.mahmud@westernsydney.edu.au](mailto:k.mahmud@westernsydney.edu.au))

12

## 13 **Abstract**

14 The lack of correlation between photosynthesis and plant growth under sink-limited  
 15 conditions is a long-standing puzzle in plant ecophysiology that currently severely  
 16 compromises our models of vegetation responses to global change. To address this puzzle,  
 17 we applied data assimilation of a simple carbon (C) balance model to an experiment where  
 18 sink strength was manipulated by restricting root volume. Our goals were to infer which  
 19 processes were affected by growth under sink limitation, and to attribute the overall reduction  
 20 in growth observed in the experiment, to the effects on component processes. Our analysis  
 21 was able to infer that, in addition to a reduction in photosynthetic rates, sink limitation  
 22 reduced the rate of utilization of non-structural carbohydrate (NSC), enhanced respiratory  
 23 losses, modified C allocation and increased foliage turnover. Each of these effects was found  
 24 to have a significant impact on final plant biomass accumulation. We also found that  
 25 inclusion of a NSC storage pool was necessary to capture seedling growth over time,  
 26 particularly for sink limited seedlings. Our approach of applying data assimilation to infer C  
 27 balance processes in a manipulative experiment enabled us to extract considerable new  
 28 information from an existing dataset. We suggest this approach could, if used more widely,



29 be an invaluable tool to develop appropriate representations of sink-limited growth in  
30 terrestrial biosphere models.

31

32 **Keywords:** Non-structural carbohydrate, carbon allocation, data assimilation, mass-balance,  
33 photosynthesis, plant growth, sink regulation

34

## 35 1 Introduction

36 Almost all mechanistic models of terrestrial vegetation function are based on the carbon (C)  
37 balance: plant growth is represented as the difference between C uptake (through  
38 photosynthesis) and C loss (through respiration and turnover of plant parts). This approach to  
39 modeling plant growth dates back to early crop and forest production models (McMurtrie and  
40 Wolf, 1983; de Wit and van Keulen, 1987; de Wit, 1978) and now provides the fundamental  
41 quantitative framework to integrate our scientific understanding of plant ecosystem function  
42 (Bonan 2008).

43 However, C balance models have been criticized for being “source-focused” (Fatichi et al.,  
44 2014). Most C balance models predict growth from the environmental responses of  
45 photosynthesis (“source limitation”). In contrast to this assumption, many experimental  
46 studies demonstrate that growth is directly limited by environmental conditions (“sink  
47 limitation”) rather than the availability of photosynthate. For example, growth is more  
48 sensitive to water limitation than is photosynthesis (Bradford and Hsiao, 1982; Müller et al.,  
49 2011; Mitchell et al., 2014); low temperatures are considerably more limiting to cell division  
50 than to photosynthesis (Körner et al., 2014); nutrient limitation may slow growth without  
51 reducing photosynthesis (Reich, 2012; Crous and Ellsworth, 2004); and, physical sink-  
52 limitation may reduce growth with a decline in photosynthetic capacity and an accumulation  
53 of leaf starch (Arp, 1991; Campany et al., 2017; Poorter et al., 2012a).

54 How can we move to models that include both source- and sink-limitation? Some C balance  
55 models include a “storage” pool of non-structural carbohydrates (NSC) (Running and Gower,  
56 1991; Bossel, 1996; Thornley and Cannell, 2000), but most of these models make the  
57 assumption that the NSC pool acts merely as a buffer between C sources and sinks, balancing



58 out seasonally or at least over several seasons (Fatichi et al., 2014; Friend et al., 2014; De  
59 Kauwe et al., 2014; Schiestl-Aalto et al., 2015). There is mounting evidence that the NSC  
60 plays a more active role in tree physiology (Buckley, 2005; Sala et al., 2012; Wiley and  
61 Helliker, 2012). For example, NSC accumulation can lead to down-regulation of  
62 photosynthesis (Nikinmaa et al., 2014). Therefore, the need to quantify the NSC pool and to  
63 better understand the prioritisation of storage vs. growth is of great importance.

64 An understanding of the dynamics of storage is also essential to correctly represent the C  
65 balance in models. If, for example, a direct growth limitation is implemented into models,  
66 how should the surplus of accumulated photosynthates be treated? In their proof-of-concept  
67 sink-limited model, Fatichi et al. (2013) allowed reserves to accumulate indefinitely.  
68 Alternatively, some models (e.g. CABLE (Law et al., 2006), O-CN (Zaehle and Friend,  
69 2010)) increase respiration rates when excess labile C accumulates. Both approaches can be  
70 seen as model-oriented solutions to maintain C balance that are unsatisfactory because they  
71 are not based on empirical data. Experiments where sink strength is manipulated may provide  
72 the key to improve our understanding of C balance processes under direct growth limitation.

73 Efforts have been made to quantify growth and understand the physiological and  
74 morphological changes in response to belowground C sink limitation by manipulating rooting  
75 volume in tree seedlings (Arp, 1991; Company et al., 2017; Poorter et al., 2012a). These  
76 experiments often reveal photosynthetic down-regulation and accumulation of leaf starch,  
77 and reductions in growth (Arp, 1991; McConnaughay and Bazzaz, 1991; Gunderson and  
78 Wullschleger, 1994; Sage, 1994; Poorter et al., 2012a; Robbins and Pharr, 1988; Maina et al.,  
79 2002; Company et al., 2017). In a recent study with Eucalyptus seedlings, Company et al.  
80 (2017) showed that the reduction in seedling growth when rooting volume was restricted  
81 could not be completely explained by the negative effects of sink limitation on  
82 photosynthesis, suggesting that other components of the C balance were affected in the  
83 process. However, Company et al. (2017) could not accurately quantify all components of  
84 tree C balance, i.e. photosynthesis, carbohydrate storage, biomass partitioning and  
85 respiration.

86 Quantifying all components of C balance is not an easy task, given that not all processes are  
87 measured with equal fidelity, and data gaps will always occur. Here, we used a data  
88 assimilation (DA)-modelling framework, which has been proven to be a powerful tool in  
89 analyzing complex C balance problems (Williams et al., 2005; Richardson et al., 2013). For



90 example, Richardson et al. (2013) use DA to discriminate among alternative models for the  
91 dynamics of non-structural carbon (NSC), finding that a model with two NSC pools, fast and  
92 slow, performed best; Rowland et al. (2014) applied DA to experimental observations of  
93 ecosystem C stocks and fluxes to infer seasonal shifts in C allocation and plant respiration in  
94 an Amazon forest; and Bloom et al. (2016) used DA to constrain a C balance model with  
95 satellite-derived measurements of leaf C, to simulate continental-scale patterns in C cycle  
96 processes.

97 Our goal in this paper was to use DA to quantify the impact of sink limitation on C balance  
98 processes. We utilized data from an experiment in which sink limitation was induced by  
99 restricting the rooting volume of *Eucalyptus tereticornis* seedlings over the course of 4  
100 months (Campany et al., 2017). We assimilated photosynthesis and growth measurements  
101 from the experiment into a simple C balance model, to infer the effects of sink limitation on  
102 the main C balance processes, namely: respiration, carbohydrate utilisation, allocation, and  
103 turnover. We first tested two null hypotheses:

104 H1: There is no need to consider storage in the model: growth can be adequately predicted  
105 from current day photosynthate.

106 H2: There is no effect of sink limitation on C balance processes other than via a reduction of  
107 photosynthesis.

108 We were then interested to test the following specific hypotheses about the impact of sink  
109 limitation on C balance:

110 H3: We hypothesized that the rate of utilization of carbohydrate for plant growth would be  
111 lower under sink limitation, causing growth rates to slow and non-structural carbohydrate to  
112 accumulate.

113 H4: We hypothesized that under sink limitation a larger proportion of C would be lost to  
114 growth respiration and less used for production. We have dubbed this the “wasteful plant”  
115 hypothesis; this hypothesis corresponds to the assumption embedded in some models that  
116 respiration is up-regulated when labile C accumulates e.g. CABLE, O-CN (Law et al., 2006;  
117 Zaehle and Friend, 2010).



H5: We hypothesized that foliage and root C allocation fractions would be reduced, in favour of wood allocation. Sink limitation induced by nutrient and/or water stress often results in a shift in C allocation away from foliage and towards fine roots (Poorter et al., 2012b). However, for this experiment, the physical restriction of root growth limits the potential for root allocation. Hence, we predicted that both foliage and fine root allocation would decrease.

## 2 Materials and Methods

### 2.1 Experiment description

The site and experimental setup have been described in detail by Campany et al. (2017), so we only provide a brief description here. The experiment was carried out at the Hawkesbury Forest Experiment site (33°37'S 150°44'E) in Richmond, NSW, Australia. Twenty-week old *Eucalyptus tereticornis* seedlings in tube stock were chosen from a single local Cumberland plain cohort. Ten seedlings were harvested at the start of the experiment to measure initial leaf area and dry mass of foliage, woody components and roots. Forty-nine seedlings were used in the main experiment, allocated to seven treatments. The plants were grown in containers of differing volume set into the ground (5, 10, 15, 20, 25 or 35 L), or were planted directly into soil (free seedlings, used as the control). All plants were grown in the open under field conditions, but were watered regularly to avoid moisture stress.

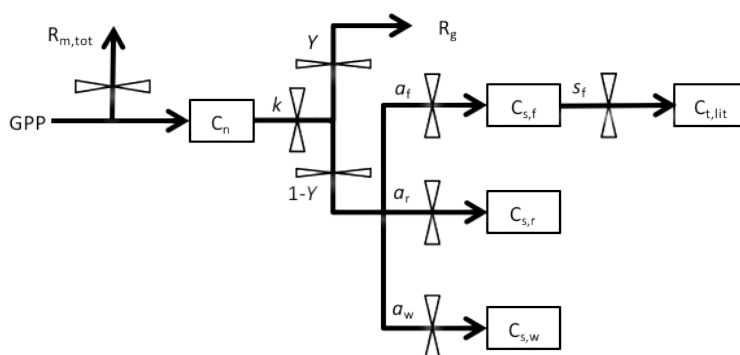
The site is located in the sub-humid temperate region which experiences warm summers and cool winters. The seedlings were planted on 21<sup>st</sup> January 2013 (mid-summer) and harvested on 21<sup>st</sup> May 2013 (late autumn). Mean daily temperatures ranged from 22.8 to 46.4 °C (monthly mean of 32.1 °C) in January 2013, which was the warmest month of the year and cooled down in May 2013 with an average of 21 °C (BoM, 2017).

### 2.2 Carbon Balance Model (CBM)

We used a DA-modelling framework, similar to that used by Richardson et al. (2013). This approach uses a simple carbon balance model shown in Figure 1. The model is driven by daily inputs of gross primary production (GPP). Total maintenance respiration,  $R_{m,tot}$ , (calculated as a temperature-dependent respiration rate,  $R_m$ , multiplied by plant biomass), is immediately subtracted, and the remainder enters a non-structural C pool ( $C_n$ ). This pool is utilized for growth at a rate  $k$  (i.e.  $kC_n$ ). Of the utilization flux, a fraction  $Y$  is used in growth



148 respiration ( $R_g$ ), and the remaining fraction ( $1-Y$ ) is allocated to structural C pools ( $C_s$ ):  
 149 among foliage, wood and root ( $C_{s,f}$ ,  $C_{s,w}$ ,  $C_{s,r}$ ). The foliage pool is assumed to turn over with  
 150 rate  $s_f$ . We assume there is neither wood or root turnover as the seedlings in the experiment  
 151 were young.



152

153 **Figure 1:** Structure of the Carbon Balance Model. Pools, shown as boxes:  $C_n$ , non-structural  
 154 storage C;  $C_{s,f}$ , structural C in foliage;  $C_{s,r}$ , structural C in roots;  $C_{s,w}$ , structural C in wood.  
 155 Fluxes, denoted by arrows, include: GPP, gross primary production;  $R_{m,tot}$ , total maintenance  
 156 respiration;  $R_g$ , growth respiration;  $C_{t,lit}$ , structural C in leaf litterfall. Fluxes are governed by  
 157 six key parameters:  $k$ , storage utilization coefficient;  $Y$ , growth respiration fraction;  $a_f$ ,  
 158 allocation to foliage;  $a_w$ , allocation to wood;  $a_r$ , allocation to roots;  $s_f$ , leaf turnover rate.

159 The dynamics of the four carbon pools are described by four difference equations:

$$\Delta C_n = GPP - R_m(C_{t,f} + C_{t,w} + C_{t,r}) - k C_n \quad (1)$$

$$\Delta C_{s,f} = k C_n (1 - Y) a_f - s_f C_{s,f} \quad (2)$$

$$\Delta C_{s,w} = k C_n (1 - Y) a_w \quad (3)$$

$$\Delta C_{s,r} = k C_n (1 - Y) (1 - a_f - a_w) \quad (4)$$

160 Where GPP is the gross primary production ( $\text{g C plant}^{-1} \text{d}^{-1}$ );  $R_m$  is the maintenance  
 161 respiration rate ( $\text{g C g}^{-1} \text{C d}^{-1}$ );  $C_{t,f}$ ,  $C_{t,w}$ , and  $C_{t,r}$  are the total C in foliage, wood and root  
 162 respectively ( $\text{g C plant}^{-1}$ );  $k$  is the storage utilization coefficient ( $\text{g C g}^{-1} \text{C d}^{-1}$ );  $Y$  is the  
 163 growth respiration fraction;  $a_f$ ,  $a_w$ ,  $a_r$  are the allocation to foliage, wood and root respectively;  
 164 and  $s_f$  is the leaf turnover rate ( $\text{g C g}^{-1} \text{C d}^{-1}$ ).

165 The non-structural (storage) C pool ( $C_n$ ) is assumed to be divided amongst foliage, wood and  
 166 root tissues ( $C_{n,f}$ ,  $C_{n,w}$ ,  $C_{n,r}$ ) according to empirically-determined fractions. The sink-limited



167 container experiment only measured leaf non-structural C ( $C_{n,f}$ ), and therefore to estimate the  
 168 partitioning of the non-structural C among different organs, we used data from a different  
 169 experiment on similar-sized seedlings of a related species (*Eucalyptus radiata*) (Duan et al.,  
 170 2013). We only considered the ambient well-watered control treatments from that  
 171 experimental dataset, and found that mass-specific  $C_n$  was distributed in the ratio 75:16:9  
 172 among foliage, wood and root pools.

173 Total carbon in each tissue ( $C_t$ ) is then calculated as the sum of non-structural carbon ( $C_n$ )  
 174 and structural carbon ( $C_s$ ) for that tissue.

$$C_{t,f} = C_{n,f} + C_{s,f} \quad (5)$$

$$C_{t,w} = C_{n,w} + C_{s,w} \quad (6)$$

$$C_{t,r} = C_{n,r} + C_{s,r} \quad (7)$$

### 175 2.3 Experimental data acquisition

176 Full details of all measurements are given in Campany et al. (2017). The mass of each pool  
 177 (foliage, wood, root, storage) was estimated over time as follows. The initial dry mass of  
 178 leaves, woods and roots was measured for 10 seedlings at the start of the experiment using  
 179 the harvesting procedure described in Campany et al. (2017). The dry mass of all  
 180 experimental plants was measured at the end of the experiment following the same procedure.  
 181 Seedling growth was tracked during the four months of the experiment, by measuring stem  
 182 height ( $h$ ), diameter at 15 cm height ( $d$ ) and number of leaves on a weekly basis. These  
 183 measurements were used to estimate the time course of wood and foliage biomass: for root  
 184 total C we used only initial and final harvest measurements. Initial root C was estimated by  
 185 averaging all 10 harvested seedlings.

186 We estimated weekly total C in wood ( $C_{s,w}$ ) from the measurements of stem height and  
 187 diameter, by using an allometric model fitted to initial and final harvest data.

$$\log(C_{t,w}) = b_1 + b_2 \log(d) + b_3 \log(h) \quad (8)$$

188 For each seedling, the total leaf area (LA) and foliage total C ( $C_{t,f}$ ) over time ( $t$ ) were  
 189 estimated based on harvested data ( $T$  = time of harvest) and weekly leaf counts (LC) over  
 190 time.

191



$$LA(t) = \frac{LA(T)}{LC(T)} LC(t) \quad (9)$$

$$C_{t,f}(t) = \frac{M_f(T)}{LC(T)} LC(t) \quad (10)$$

192 Fully expanded new leaves were sampled for total non-structural carbohydrate (NSC)  
 193 concentration on a fortnightly basis. These concentrations were multiplied by leaf biomass to  
 194 estimate the foliage TNC pool ( $C_{n,f}$ ) at each time point. The partitioning of the non-structural  
 195 C amongst foliage, wood and root tissues (75:16:9) was then used to estimate the wood and  
 196 root components of the total TNC pool. Structural C mass for each component was estimated  
 197 by subtracting non-structural C mass from total C mass.

198 We estimated daily GPP from leaf-level gas exchange measurements and a simple canopy  
 199 scaling scheme as described in Company et al. (2017), and summarized below.  
 200 Photosynthetic  $CO_2$  response (ACi) curves and leaf dark respiration rates (R) were measured  
 201 on two occasions, 13-14<sup>th</sup> March 2013 (when new leaves were first produced) and 14-15<sup>th</sup>  
 202 May 2013 (prior to the final harvest). The ACi curves were used to estimate photosynthetic  
 203 parameters (the maximum rate of Rubisco carboxylation,  $V_{cmax}$  and the maximum rate of  
 204 electron transport for RuBP regeneration under saturating light,  $J_{max}$ ) using the biochemical  
 205 model of Farquhar et al. (1980) and fit with the ‘plantecophys’ package (Duursma, 2015) in  
 206 R. The parameter  $g_1$ , reflecting the sensitivity of stomatal conductance ( $g_s$ ) to the  
 207 photosynthetic rate, was estimated by fitting the optimal stomatal conductance model of  
 208 Medlyn et al. (2011) to measured stomatal conductance data.

209 Daily net C assimilation per unit leaf area ( $C_{day}$ ) was then estimated by using a coupled  
 210 photosynthesis–stomatal conductance model (Farquhar et al., 1980; Medlyn et al., 2011)  
 211 using mean photosynthetic parameters ( $J_{max}$ ,  $V_{cmax}$ ,  $g_1$  and  $R_d$ ) for each treatment and  
 212 meteorological data from the onsite weather station. The daily GPP was estimated by  
 213 multiplying  $C_{day}$ , total leaf area (LA) and a self-shading factor. The self-shading factor, which  
 214 is a linear function of LA, is calculated by via simulation with a detailed radiative transfer  
 215 model, the ‘YplantQMC’ R package of Duursma (2014) for individual treatment. The leaf  
 216 maintenance respiration rate ( $R_m$ ,  $g\ C\ g^{-1}\ C\ plant\ d^{-1}$ ) was calculated for each seedling by  
 217 scaling the measured rate (R) to air temperature using a  $Q_{10}$  value of 1.86 (Company et al.,  
 218 2017).





## 2.4 Application of Data Assimilation (DA) algorithm

DA was used to estimate the six parameters ( $k$ ,  $Y$ ,  $a_f$ ,  $a_w$ ,  $a_r$ ,  $s_f$ ) of the CBM for this experiment. All parameters were allowed to vary quadratically with time, i.e. each parameter was represented as:

$$p = p_1 + p_2 t + p_3 t^2 \quad (11)$$

Quadratic variation over time was found to yield significantly better model fits than either constant parameter values or linear variation over time (see supplementary section S1). We executed three distinct sets of model simulations (Table 1), with the goals of (1) testing the need for a storage pool; (2) determining the effect of sink limitation on model parameters; and (3) attributing the overall effect of sink limitation on growth to the change in individual parameters.

For each set of model simulations, GPP and  $R_m$  were used as inputs to the DA framework, and the measurements of total C mass of each of the plant components and foliage NSC concentrations were used to constrain the parameter values. The set of constraints included 18 measurements of  $C_{t,f}$  and  $C_{t,w}$ , two measurements of  $C_{t,r}$  (start and end of the experiment), and six measurements of foliage NSC.

We used the Metropolis algorithm (Metropolis et al., 1953) as implemented by Zobitz et al. (2011), with broad prior Probability Density Functions (PDFs) for the parameters (Table 2). Values of  $k$ ,  $a_f$ ,  $a_r$  and  $s_f$  were allowed to vary within the maximum possible range, while parameter  $Y$  was constrained according to the literature on growth respiration (Villar and Merino, 2001). Parameter  $a_r$  was calculated from  $a_f$  and  $a_w$  with a check on  $a_r$  to ensure that it had reasonable values ( $0 < a_r < 1$ ). Standard Error (SE) was used as an estimate of uncertainty on the assimilated data (Rowland et al., 2014; Richardson et al., 2010), and was calculated based on six replicate measurements. When combining errors (e.g. Eq. 9, 10), the errors were assumed to be uncorrelated (Hughes and Hase, 2010).

The step size for the DA was set to a random draw from a normal distribution, with a mean of 0 and a SD of 0.005 in log-normal space, resulting in an acceptance rate of 35–40%. We confirmed the chain convergence, having 3000 iterations to adequately explore the posterior parameter space, by visual inspection of the trace plots of different parameters as suggested by Van Oijen (2008).



248 **Table 1:** Summary of the three model simulation sets

Simulation Set	Goal	Features	Addressing hypothesis
A	Test importance of storage pool	<ul style="list-style-type: none"> <li>• DA applied to estimate parameters for model without storage pool and model with storage pool</li> <li>• Three treatment groups</li> <li>• Not constrained with NSC data</li> <li>• No leaf area feedback</li> </ul>	H1
B	Identify effect of sink limitation on model parameters	<ul style="list-style-type: none"> <li>• DA applied to estimate parameters for model with storage pool</li> <li>• Data divided into one, two, three or seven treatment groups</li> <li>• Constrained with NSC data</li> <li>• No leaf area feedback</li> </ul>	H2-H5
C	Attribute overall effect on growth to changes in individual parameters	<ul style="list-style-type: none"> <li>• Forward model runs to quantify impact of individual processes on overall plant growth</li> <li>• 5L &amp; free seedlings considered</li> <li>• Parameters changed one at a time</li> <li>• Leaf area feedback</li> </ul>	

249 **Table 2:** Prior parameter PDFs (with uniform distribution) and the starting point of the  
250 iteration for all parameters

Parameter	Minimum	Maximum	Starting value
$k$	0	1	0.5
$Y$	0.2	0.4	0.3
$a_f$	0	1	0.5
$a_w$	0	1	0.5
$s_f$	0	0.01	0.005
$a_r = 1 - (a_f + a_w)$ , where $0 < a_r < 1$			



#### 251    **2.4.1    Importance of storage pool**

252    We tested the hypothesis (H1) on the importance of including a non-structural C storage pool  
253    in CBM by contrasting fits of the full model with fits of a simplified model without the non-  
254    structural C pool (Simulation Set A, Table 1). The simplified model omits the non-structural  
255    C pool ( $C_s$ ) from the full model (Figure 1) and assumes that all available C is utilized for  
256    growth each day. We applied the DA framework to both model options and calculated the  
257    Bayesian Information Criterion, BIC (Schwarz, 1978) to determine the better model structure.  
258    BIC measures how well the model predicts the data based on a likelihood function and  
259    compare model performance taking into account the number of fitted parameters, with the  
260    lowest BIC number indicating the best model setting. For this comparison, both models were  
261    fit to the biomass data only, not leaf NSC data, in order to ensure that both models were fit to  
262    the same number of data points.

#### 263    **2.4.2    Effects of sink limitation on model parameters**

264    The effects of sink limitation on C balance were investigated by applying the DA framework  
265    to data from all treatments combined, and then subsets of treatments (Simulation Set B, Table  
266    1). Considering all treatments pooled together gives same parameters for all the treatments  
267    and effectively assumes no effect of sink limitation. On the other hand, taking more subsets  
268    of treatments produces more parameter sets (one for each subset) and allows for parameters  
269    to vary according to the degree of sink limitation. We first fitted the model to all data,  
270    ignoring treatment differences; then considered 2 treatment groups (free seedling / 5-35 L  
271    containerized seedlings), 3 groups (free / 5-15 L / 20-35 L) and 4 groups (free / 5-10 L / 15-  
272    20 L / 25-35 L). We also fitted the model to each of the 7 treatments individually, where the  
273    parameter set for each treatment is unique. The BIC values were compared across treatment  
274    groupings.



### 275 2.4.3 Attribution analysis

276 We performed a sensitivity analysis to quantify the impact of the response of each individual  
 277 process to sink limitation on overall plant growth (Simulation Set C, Table 1). This analysis  
 278 consisted of forward runs of the model, including a leaf area feedback to GPP. That is, rather  
 279 than taking GPP based on measured LA (Eq. 9) as input, in this version of the model we  
 280 calculated daily GPP using the modelled LA, the photosynthesis rate and corresponding self-  
 281 shading factor. Adding the LA feedback to the model was necessary to quantify how the  
 282 treatment effect on individual model parameters affects final seedling biomass through its  
 283 effect on foliage mass, and consequently GPP, over time.

284 LA in each time step is estimated from NSC-free specific leaf area ( $SLA_{nonsc}$ ) and the  
 285 predicted foliage structural carbon ( $C_{s,f}$ ) in that time step.  $SLA_{nonsc}$  is calculated at harvest  
 286 discarding the foliage NSC portion and is assumed to be constant for a given treatment  
 287 throughout the experiment.

$$LA = SLA_{nonsc} \times C_{s,f} \quad (12)$$

288 Once the LA feedback was implemented in the CBM, we ran the model with the inputs and  
 289 modelled parameters from the smallest pot seedling (5 L), then changed the parameters to  
 290 those for the free seedling one at a time to quantify the effect of each parameter on the final  
 291 seedling biomass. The parameters we considered for the sensitivity test were: daily  
 292 photosynthetic rate per unit leaf area ( $C_{day}$ ), maintenance respiration rate ( $R_m$ ), C allocation  
 293 fractions to biomass ( $a_f$ ,  $a_w$ ,  $a_r$ ), growth respiration rate ( $Y$ ), foliage turnover rate ( $s_f$ ) and  
 294 utilization coefficient ( $k$ ).



295

## 296 **3 Results**

### 297 **3.1 Importance of storage pool**

298 First, we tested the null hypothesis (H1) that there is no need for a non-structural  
299 carbohydrate storage pool in the carbon balance model. We compared BIC values for model  
300 structures with and without a storage pool. Table 3 (Simulation Set A) shows the results for  
301 model fits with the optimal grouping strategy (three treatment groups). BIC values were  
302 consistently lower for the model including the storage pool; the improvement in model fit is  
303 most noticeable for the containerized seedlings. This analysis demonstrates that the model  
304 does need to include a storage pool to correctly represent the experimental data. In all  
305 remaining analyses, the full CBM (with non-structural C pool) is applied to data from all four  
306 plant C pools (NSC, foliage, wood and root biomass).

### 307 **3.2 Sink limitation effect on C balance processes**

308 We addressed our second null hypothesis (H2), that there is no effect of sink limitation on  
309 carbon balance processes, by comparing BIC values obtained for model fits when all  
310 treatments were combined vs separating the treatments into sub-groups. If there was no effect  
311 of sink limitation, the BIC value when all treatments are fit together would be similar to that  
312 obtained when treatments are separated into groups. The BIC values shown in Table 3  
313 (Simulation Set B) decrease strongly as number of treatment groups increases, indicating a  
314 clear effect of sink limitation on carbon balance processes. Although the BIC values continue  
315 to decrease as more treatment groups are considered, we also found that interpreting  
316 parameter changes became more difficult as the number of groups increased. Hence, further  
317 analyses in this paper used unique parameter sets for three treatment groups: small containers,  
318 large containers, and free seedlings.



**Table 3:** BIC values from model fits. The lowest BIC values (in bold) indicate the best performing parameter settings for any particular simulation. Note that, for Sim A, leaf NSC data were not used to constrain either model, to ensure that both models were fit to the same dataset, resulting in lower BICs compared to Sim B. Treatment groups are: ‘Small’ - 5 L, 10 L and 15 L containers; ‘Large’ - 20 L, 25 L and 25 L containers; ‘Free’ – freely rooted seedlings; ‘All’ - all data; ‘Containerized’ - all plants in containers.

Simulation Set	Model Setting	Treatment groups	BIC
Sim A	Model without storage pool	Small	459
		Large	550
		Free	182
	Model with storage pool	Small	215
		Large	338
		Free	167
Sim B	7 treatments combined	All	2768
	2 groups	Containerized	1813
		Free	170
		Total	1983
	3 groups	Small	683
		Large	457
		free	170
		Total	1310
	7 treatments individually	5 L	85
		10 L	98
		15 L	60
		20 L	63
		25 L	106
		35 L	152
		Free	170
		Total	734

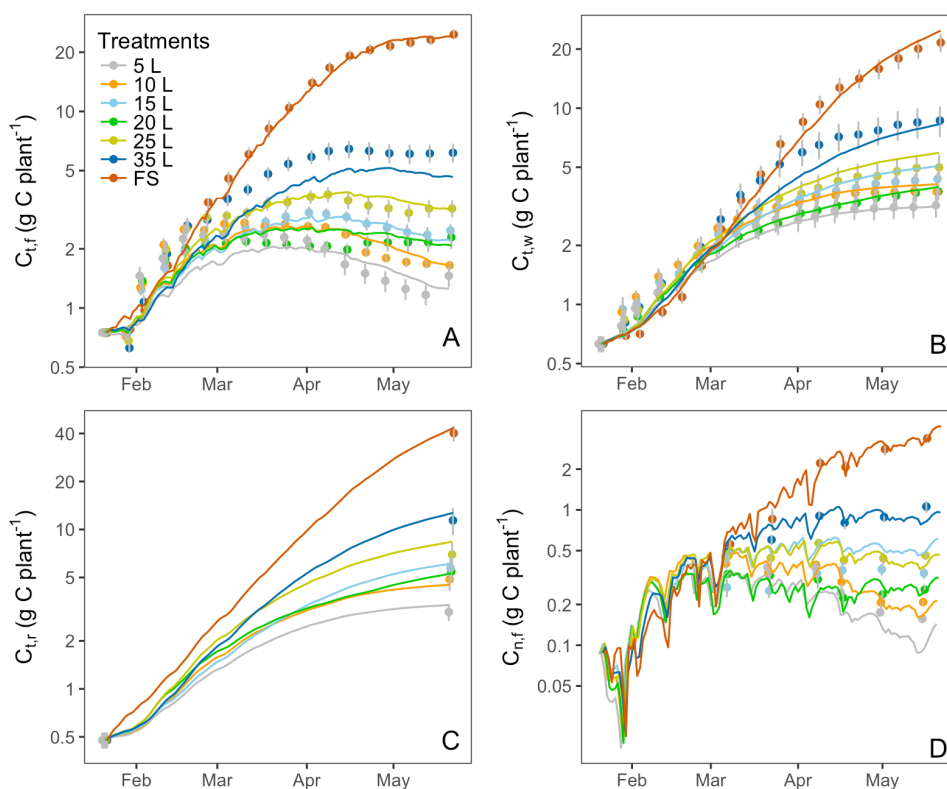
### 3.3 Analysis of carbon stock dynamics

Figure 2 shows the correspondence between modeled C pools and data. The model reproduced the key features of biomass growth over time in response to treatment. Biomass growth (Figure 2A, B and C) and the foliage storage pool (Figure 2D) were very clearly impacted by sink limitation: biomass growth was strongly reduced for containerised seedlings, which was very well mimicked by the model. Foliage growth in the free seedlings slowed towards the end of the experiment. Wood and root growth continued throughout the



experiment in freely-rooted seedlings but slowed down during the second half of the  
 experiment in containerized seedlings. In March, at the time of the first leaf NSC  
 measurements, the foliage storage pool (Figure 2D) was similar in size across all treatments,  
 but it increased over time in the free seedlings as these plants continued to grow, and  
 decreased over time in the plants in small containers.

Modelled C stocks for all 7 treatments closely tracked their corresponding observations  
 (Figure 2) as most of the predicted biomass values were within one standard error of the  
 measurements. The exception is the 35 L container treatment, which is underestimated  
 slightly because the grouping of 20, 25 and 35 L treatments into one group makes it difficult  
 for the model to fit all treatments in this group.



343

344 **Figure 2:** Modelled C stocks (lines) with optimum parameter settings and corresponding  
 345 observations (symbols): (A) total C mass in foliage  $C_{t,f}$ , (B) total C mass in wood  $C_{t,w}$ , (C)  
 346 total C mass in root  $C_{t,r}$  and (D) total C mass in foliage NSC  $C_{n,f}$ . Note that the carbon pools



(y-axes) are plotted on log scale to visualize the changes at the beginning of the experiment.  
Error bars (1 SE,  $n = 6$ ) are shown for each observation.

349

### 3.4 Parameter estimates

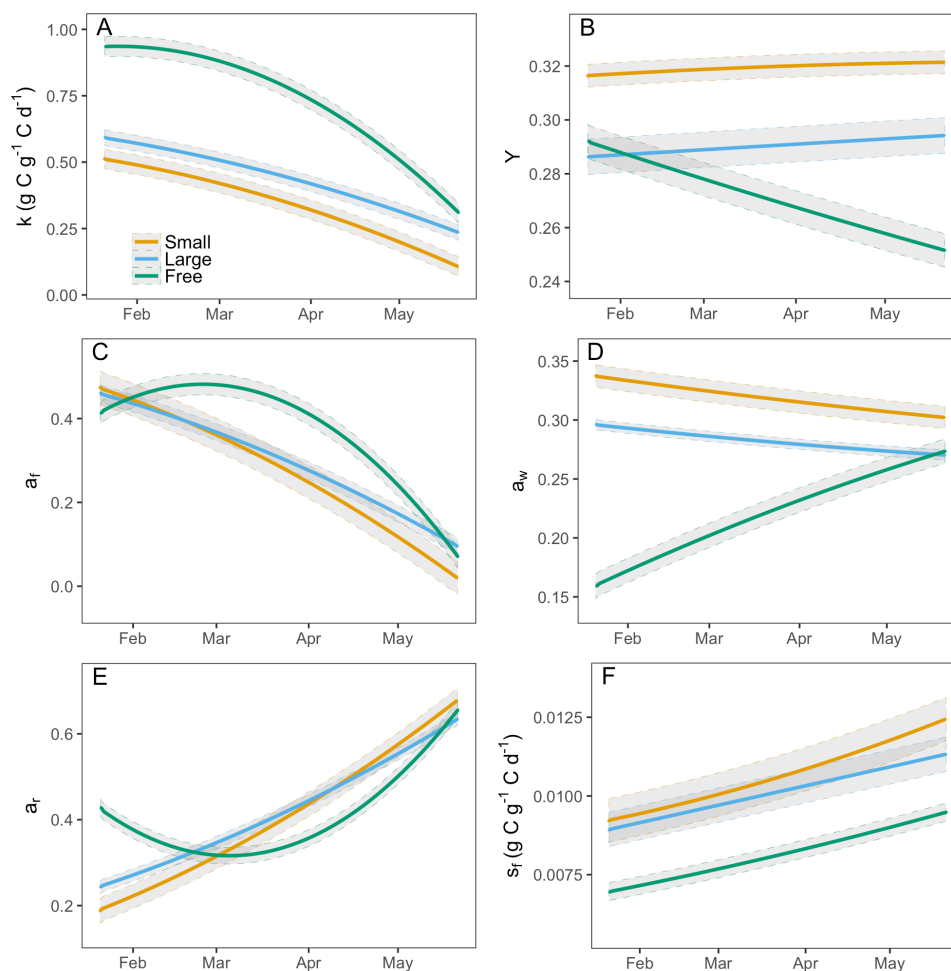
Data assimilation indicated significant treatment effects on all five fitted parameters (Figure 3). There was a large effect of sink limitation on the utilization coefficient ( $k$ ). In agreement with our hypothesis H3, the free seedling had the highest  $k$ , and the seedlings in small containers (most sink limited) had the lowest  $k$  (Figure 3A). As the experiment progressed, the utilization rate of free seedlings began to decrease (Figure 3A). In contrast to the free seedlings, the potted seedlings had relatively low utilization rates initially ( $k$  close to 0.5) and the utilization rates slowed down abruptly with time, most significantly in the smallest container treatments (Figure 3A).

In agreement with hypothesis H4, the estimated growth respiration rate ( $Y$ ) varied according to the sink strength of the treatment groups, and was highest in the lowest sink strength treatments (Figure 3B). Moreover,  $Y$  did not vary significantly over time for the sink limited treatment groups. However, the rate of growth respiration for the free seedling slowed down over time.

The data assimilation process also indicated that the growth allocation fractions vary among treatments and over time. Consistent with hypothesis H5, wood allocation fraction was highest in the smallest container treatments, and lowest in the free seedlings (Figure 3D). For the free seedlings, allocation was initially highest to foliage and roots (Figure 3C-E); over time, the plants reduced allocation to foliage and increased it to wood and roots. In the containerized seedlings, allocation was initially highest to wood and foliage; over time, foliage allocation decreased to almost zero and root allocation increased.

The estimated leaf turnover rate,  $s_f$  was also notably higher for sink-limited treatments compared to free seedlings (Figure 3F). The large value of modelled leaf litterfall for sink-limited treatments is consistent with observations during the experiment that containerized seedlings had relatively large leaf litterfall, beyond normal senescence. Estimated  $s_f$  increased over time for all treatment groups (most notably in free seedlings), due to a combination of ontogeny, seasonal change, and growth restriction in the sink-limited seedlings.





377

378 **Figure 3:** Modelled final parameters for three groups of treatments during the experiment  
 379 period (21st Jan to 21st May 2013): (A) storage utilization coefficient,  $k$ ; (B) growth  
 380 respiration fraction,  $Y$ ; (C) allocation to foliage,  $a_f$ ; (D) allocation to wood,  $a_w$ ; (E) allocation  
 381 to roots,  $a_r$  and (F) leaf turnover rate,  $s_f$ . The grey shaded area shows the 95% confidence  
 382 intervals of modelled parameters.

383

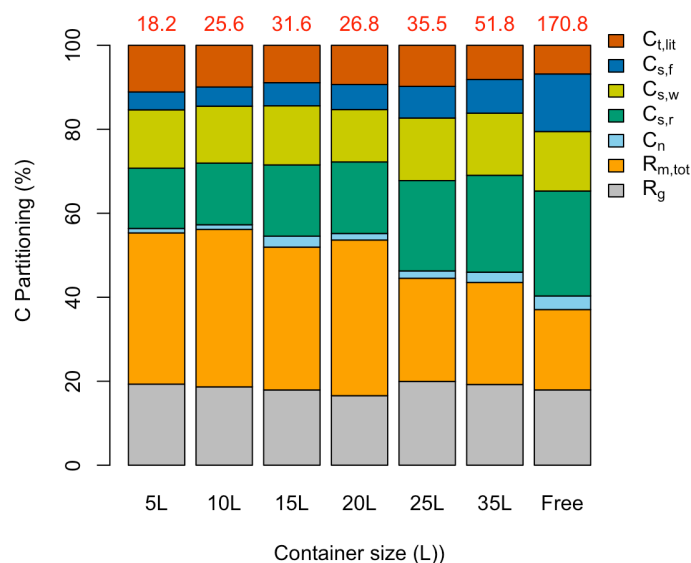
### 384 3.5 Carbon budget

385 The model was used to partition total GPP ( $\text{g C plant}^{-1}$ ) from the entire experiment period  
 386 into different C pools (growth respiration, maintenance respiration, non-structural carbon,  
 387 structural foliage, wood, and root carbon, and litterfall) for all 7 treatments (Figure 4). Total



388 GPP was considerably lower for the containerized seedlings, owing to lower photosynthetic  
389 rates per unit leaf area,  $C_{\text{day}}$  (Figure 5A), and lower total leaf area (LA) per plant. Though  
390 starting with the same total LA of  $0.016 \text{ m}^2$ , the 5 L containerized and free seedlings had total  
391 LA of  $0.031$  and  $0.516 \text{ m}^2$  respectively after four months of treatment. Simultaneously, the  
392 partitioning of GPP changed considerably across different treatments.

393 Small container seedlings (5, 10, 15 L) had a higher fraction of GPP lost in leaf litterfall  
394 compared to other seedlings (Figure 4), consistent with observations during the experiment.  
395 The proportion of GPP in final foliage mass was extremely low in sink limited treatments  
396 (also shown in Figure 2A). Allocation of GPP to final foliage and root biomass were highest  
397 in the free seedlings, although interestingly allocation to final wood biomass was similar  
398 across treatments. The final allocation to storage was also higher in free seedlings. The sink  
399 limited seedlings had a higher proportional C lost through maintenance respiration. Tissue  
400 specific respiration rates were similar in free and containerized seedlings, so the ~35%  
401 reduction in photosynthetic rate for the smallest containerized seedling, led to a higher overall  
402  $R_{\text{m,tot}}/\text{GPP}$  fraction. In summary, the estimated total respiration ( $R_{\text{m,tot}} + R_g$ ) to GPP ratio was  
403 considerably lower for the free seedlings compared to the sink limited treatments.



404

405 **Figure 4:** Proportional C partitioning for the whole experimental period. The total  
 406 accumulated GPP (g C plant<sup>-1</sup>) for individual treatments is shown (in red) at the top of each  
 407 column. Free stands for free seedling. Different C partitions are in the colour legend: total  
 408 litterfall,  $C_{t,lit}$ ; foliage structural C,  $C_{s,f}$ ; wood structural C,  $C_{s,w}$ ; root structural C,  $C_{s,r}$ ; non-  
 409 structural C pool,  $C_n$ ; total maintenance respiration,  $R_{m,tot}$  and growth respiration,  $R_g$ .

410

### 411 3.6 Attribution analysis

412 Sink limitation affected biomass growth via a range of processes, namely reduction in  
 413 photosynthesis, and variation in the utilization rate, growth respiration, leaf litterfall, and C  
 414 allocations to foliage, wood and root across various treatment groups. We quantified the  
 415 contribution of each of these process responses separately by running the CBM with  
 416 parameter inputs changing one at a time. This analysis attempts to attribute the change in  
 417 biomass between the smallest container treatment (5 L) and the free seedlings to the  
 418 underlying mechanisms. Figure 5 shows how biomass ( $M_f$ ,  $M_w$  and  $M_r$ ) is predicted to change  
 419 due to each parameter change from 5 L container (gray line, Figure 5) to free seedling (red  
 420 line, Figure 5). Different colours in the figure indicate the parameter shifts (left column, A-F)



421 and their associated impacts on C budgets (right column, G-I). Final biomass values are given  
 422 in Table 4.

423 Daily net C assimilation per unit leaf area ( $C_{\text{day}}$ ), which was 30% higher for free seedling  
 424 compared to 5 L container treatment (Figure 5A), had a large impact on plant growth (final  
 425 total biomass was increased by 11 g, Table 4 and Figure 5G-I, gray to orange). Maintenance  
 426 respiration rate ( $R_m$ ) did not vary significantly across treatments (Figure 5B), in line with the  
 427 data presented in Campany et al. (2017), and consequently its impact was insignificant (the  
 428 final total biomass is reduced by only 0.2 g, Table 4 and Figure 5G-I, orange to light blue).  
 429 The modelled biomass allocation fractions ( $a_f$ ,  $a_w$  and  $a_r$ ) in Figure 5C had important, but  
 430 mixed, effects on C stocks. The final foliage mass was increased from 2.54 g to 6.62 g due to  
 431 the increase in C allocation to foliage (Table 4 and Figure 5G, light blue to green), which has  
 432 a positive feedback on GPP. Concomitant changes in C allocation to wood and root resulted  
 433 in smaller changes to these biomasses as shown in Figure 5H-I (1.34 g and 4.47 g rise  
 434 respectively, Table 4). Overall, the change in allocation pattern resulted in an increase in final  
 435 total biomass by 9.9 g. Growth respiration rate ( $Y$ ) was ~20% lower in free seedlings (Figure  
 436 5D), which had a considerable impact on C budgets (the final total biomasses were increased  
 437 by 6.1 g, Table 4 and green to yellow, Figure 5G-I). Leaf turnover,  $s_f$  was low in the free  
 438 seedlings compared to the 5 L container treatment (Figure 5E) which had a large positive  
 439 effect on final C pools (yellow to blue, Figure 5G-I). The foliage mass was increased by 3.76  
 440 g; the wood and root masses were also further increased (2.27 g and 3.87 g respectively) due  
 441 to the increase in GPP when foliage is retained for longer. Finally, the utilization coefficient,  
 442  $k$  was higher in free seedlings (Figure 5F) causing a 20-30% positive feedback on C budgets  
 443 (total biomass increased by 13.2 g, Table 4 and blue to red, Figure 5G-I).

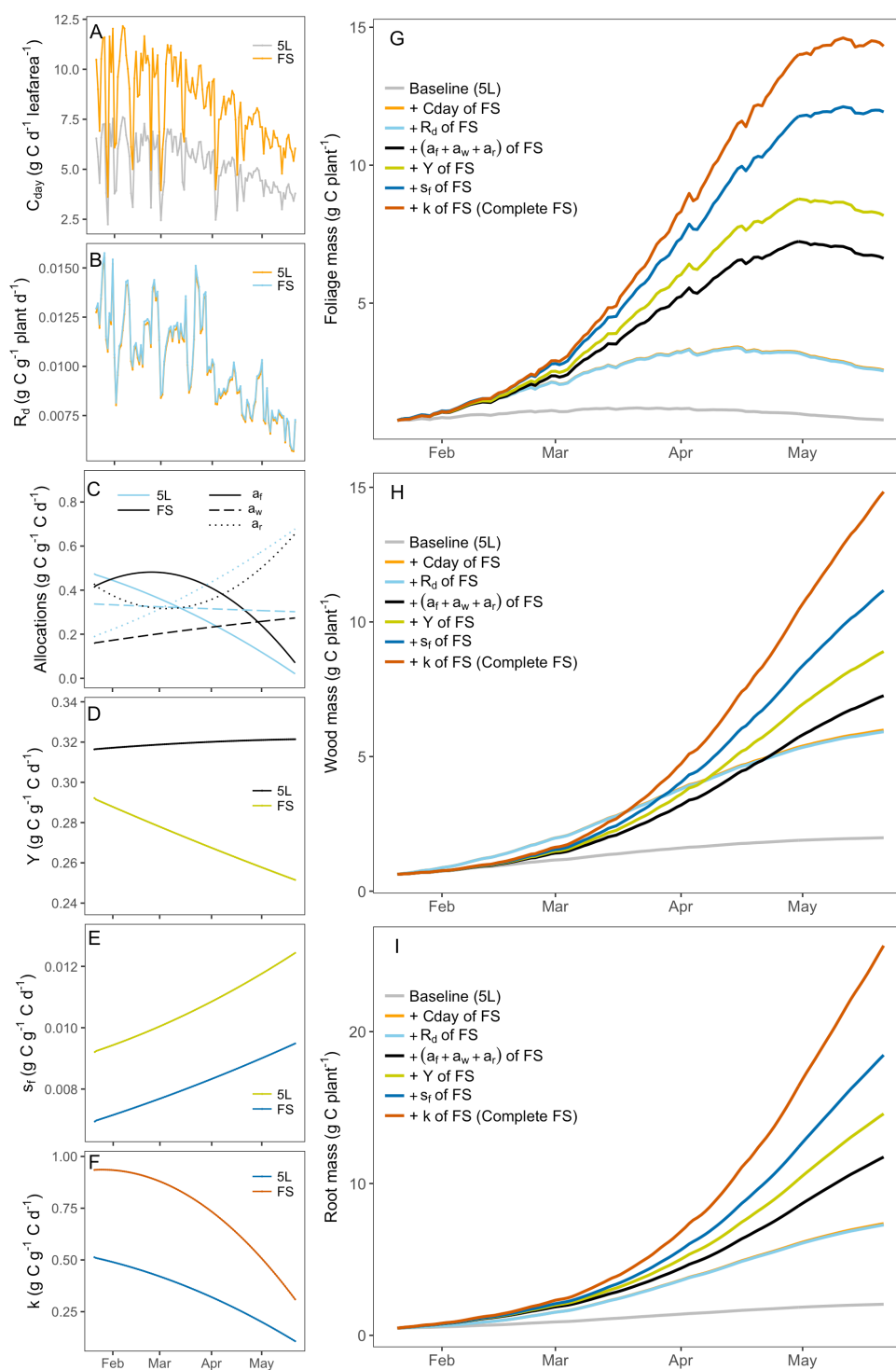




**Figure 5:** Attribution analysis. Left column (A-F): changes in input parameters; Right column (G-I): associated impacts on C budgets (right column, G-I). Colours indicate different parameters. Legend: 5L, highly sink-limited treatment with container size of 5 L; FS, Free Seedling without any sink limitation. Note that the orange line is overlain by the light blue line: the small change in maintenance respiration results in a very minor effect on biomass growth.

**Table 4:** Estimates of final biomass due to individual parameter change, showing the contributions to overall change in biomass. All values in g C plant<sup>-1</sup>. Different columns represent C partitioning to total foliage, C<sub>t,f</sub>, total wood, C<sub>t,w</sub>, total root, C<sub>t,r</sub>, and the sum of total plant C, C<sub>t</sub>.

	C <sub>t,f</sub>	C <sub>t,w</sub>	C <sub>t,r</sub>	C <sub>t</sub>
5 L (Baseline)	0.77	1.98	2.05	4.8
+ C <sub>day</sub>	2.57	5.98	7.36	15.9
+ R <sub>d</sub>	2.54	5.92	7.27	15.7
+ (a <sub>f</sub> + a <sub>w</sub> + a <sub>r</sub> )	6.62	7.26	11.74	25.6
+ Y	8.17	8.90	14.59	31.7
+ S <sub>f</sub>	11.93	11.17	18.46	41.6
+ k	14.32	14.83	25.66	54.8

## 4 Discussion

### 4.1 Effects of sink limitation on C balance

Our DA-model analysis of this root volume restriction experiment provided significant new insights in the response of key C balance processes to sink limitation. We were able to infer that, in addition to a reduction in photosynthetic rates, sink limitation reduced NSC utilization rates, increased growth respiration, modified allocation patterns and enhanced senescence. Our attribution analysis indicated that all of these process responses contributed significantly to the overall reduction in biomass observed under low rooting volume.

We first tested the null hypothesis (H1) that seedling growth rates could be adequately predicted from current-day photosynthate. This hypothesis was rejected, with a storage pool being necessary to simulate growth, particularly for containerized seedlings (Sim A, Table 3).



467 The approach of simulating growth from current-day photosynthate is commonly used in  
468 models, particularly for evergreen plants (e.g. (Jain and Yang, 2005; Law et al., 2006;  
469 Thornton et al., 2007)), but several authors have proposed the need for a storage pool to  
470 balance the C sources and sinks in the short term, as well as simulate the effects of  
471 photosynthetic down-regulation in the long-term (Pugh et al., 2016; Richardson et al., 2013).  
472 Our results support the need for an NSC pool in CBMs.

473 We then tested the second null hypothesis (H2) that there was no effect of treatment on the  
474 parameters of the C balance model. This hypothesis was also rejected: fitting the DA-model  
475 framework simultaneously to all treatments with one set of parameters (ignoring sink  
476 limitation effect) gave a low goodness of fit (Sim B, Table 1). This result is consistent with  
477 the finding of Campany et al. (2017) that the observed effects of sink limitation on  
478 photosynthesis in this experiment were insufficient to explain the large reduction in biomass.  
479 Instantaneous photosynthetic rates were reduced 20-30% by sink limitation. The C balance  
480 model was driven with daily photosynthesis values derived from these measurements. Had  
481 the reduction in growth been due solely to photosynthesis, other parameters to the model  
482 would have been similar across treatments. Instead, our DA analysis indicated that several  
483 other processes contributed to the reduction in biomass growth, including carbohydrate  
484 utilization, growth respiration, allocation patterns, and turnover.

485 Our results suggested a significant effect of sink limitation on the carbohydrate utilization  
486 rate,  $k$  (Figure 3A). The modelled  $k$  values were approximately twice as high in free seedlings  
487 compared to the small containers. This result supports the hypothesis (H3) that plants would  
488 have the lowest utilization rate under sink-limited conditions. At the start of the measurement  
489 period, the free seedlings were utilizing almost all C produced immediately in growth ( $k$  close  
490 to 1.0, Figure 3A), partially supporting the hypothesis H2. However, introducing a storage  
491 pool in the model improved the DA-modelling results for the entire experimental period,  
492 emphasizing the importance of C partitioning to storage and rejecting the hypothesis H2. The  
493 utilization coefficient of the free seedlings decreased over time, causing a build-up of C  
494 storage (Figure 2D). This decrease in utilization rate could potentially be an ontogenetic  
495 effect, with free seedlings initially allocating all carbon to growth during establishment but  
496 increasing storage with increasing size. However, ontogenetic effects are confounded with  
497 season in this experiment, such that decreasing utilization rates over time could also be a  
498 result of decreasing temperatures moving into autumn. There is a real need to quantify how



499 the carbohydrate utilization rate varies with environmental conditions and ontogeny; data  
500 assimilation of experiments in which photosynthesis and growth rates have been monitored  
501 over time offer one means to do so.

502 Although the carbohydrate utilization rate was highest in the free seedlings, leaf carbohydrate  
503 concentrations were not lower in these plants at the end of the experiment. As shown in the  
504 final C budget analysis (Figure 4), there was a higher total C allocation to the NSC pool in  
505 free seedlings than sink-limited treatments. Final carbohydrate storage was high in free  
506 seedlings despite high  $k$  because the carbohydrate pool was recharged throughout the  
507 experiment (Figure 2D), as the free seedlings had high photosynthetic rates but no higher  
508 maintenance respiration requirement. In contrast, NSC was depleted for the smallest pot  
509 treatments after mid-March (Figure 2D) when demand exceeded supply due to both limited  
510 production of photoassimilates and enhanced leaf litterfall (Figure 3F).

511 The modelled rate for growth respiration,  $Y$  was larger for sink limited treatments than the  
512 free seedling (Figure 3B). This finding supports the “wasteful plant” hypothesis H4. Inferred  
513  $Y$  remained constant over time for the containerized treatments, implying a fixed portion of C  
514 loss due to growth respiration despite seasonal variation. However, a reduction in  $Y$  over time  
515 was inferred for the free seedling, suggesting a possible ontogenetic effect. However, it is  
516 important to note that we have inferred growth respiration from the CBM framework.  
517 Therefore, these estimates could possibly also include C losses via other pathways. Direct  
518 measurements of growth respiration rates would be useful to confirm the inferred effects of  
519 sink limitation and investigate potential underlying mechanisms.

520 We also demonstrated that the allocation fractions among organs change in sink-limited  
521 conditions, with sizeable consequences for plant growth rates. There were significant  
522 variations among treatments in the modelled C allocation fractions to foliage, wood and root;  
523 modelled allocation fractions also varied significantly over time (Figure 3C, D and E). At the  
524 beginning of the experiment, foliage allocation fractions were similar for all treatment  
525 groups, but wood allocation was higher, and root allocation lower, in the containerized  
526 seedlings compared to the free seedlings. Over time, allocation to foliage in the free seedlings  
527 decreased, and allocation to both wood and roots increased, likely reflecting ontogenetic  
528 effects. For the containerized seedlings, foliage allocation declined steeply over time, while  
529 wood allocation decreased marginally and root allocation increased steeply. These allocation





530 patterns supported our hypothesis H5 that sink limitation due to root restriction would favour  
531 allocation to wood over foliage or fine roots.

532 The inferred biomass allocation pattern was also supported by the final biomass partitioning  
533 from DA (Figure 4). The C partitioning to final foliage and root mass was proportional to  
534 sink strength. The effect of sink limitation on foliage allocation adds further quantitative  
535 information to the relatively scarce data in literature and opposes the review of Poorter et al.  
536 (2012a) that summarizes no effect of foliage partitioning. On the other hand, more evidence  
537 is present on root partitioning with contrasting evaluation. Our finding supports Hess and De  
538 Kroon (2007), expecting root allocation to decrease in smaller containers. However, in  
539 contrast NeSmith and Duval (1998) did not find any differences with sink strength and  
540 Poorter et al. (2012a) reviewed that over ~80 species and experiment combinations, root  
541 allocation decreased 4% on average with a doubling in sink size. This conflicting variation in  
542 responses might be the result of differences in age of plants, species and even between  
543 cultivars within a species considered in various experiments (Poorter et al., 2012a; NeSmith  
544 and Duval, 1998). Our DA analysis shows potential drop in root allocation due to the  
545 physical restriction of root development with the growth of sink limited seedlings. Moreover,  
546 DA shows the proportion of C in wood biomass did not vary for sink limitation, supporting  
547 the outcome of Poorter et al. (2012a). All these changes in C allocation pattern support the  
548 hypothesis H5, stating both foliage and root allocations reduced in response of sink  
549 limitation. However, these reductions happened not in favour of wood allocation but to  
550 maintain the respiratory losses of sink limited seedlings. Overall, there was lower C utilization  
551 in plant structural growth in sink limited treatments (~45%) compared to free seedling  
552 (~60%).

#### 553 4.2 Application of DA to infer C balance processes

554 We have demonstrated that the DA approach can be an invaluable tool for quantifying C  
555 fluxes in experimental systems, enabling us to extract important new information from  
556 existing datasets to inform carbon balance models, such as the rate and timing of the transfer  
557 of photosynthate to and from storage pools. We applied a DA-modelling framework to a  
558 belowground sink limitation experiment (Campany et al. 2017). The experimental data  
559 showed that the reduction of seedling growth under sink limitation was not completely  
560 explained by the drop in C assimilation, suggesting that other C balance processes were also  
561 responsible for the growth reduction. However, the experimental measurements did not



562 directly quantify all the C balance components involved (Campany et al., 2017). The DA-  
563 modelling approach is able to draw together the experimental data to estimate all the  
564 components of C balance, including photosynthesis, respiration, NSC, biomass partitioning  
565 and turnover. This approach could readily be applied to other experiments to derive new  
566 information allowing better representation of C balance processes in vegetation models.

567 Applying this approach requires a range of measurements to constrain the key C balance  
568 processes. Here, we used estimated daily C assimilation and maintenance respiration rate as  
569 model inputs and constrained the model with measurements of biomass pools (foliage, wood,  
570 root) and foliage NSC concentrations. We used fortnightly foliage and wood biomass  
571 measurements; the DA framework would work with fewer data observations, but parameters  
572 would be estimated with less accuracy. Informal exploration of the model suggested that  
573 measurements of foliage turnover would have been particularly useful to better constrain the  
574 model. Any experiment having estimates of GPP, maintenance respiration, and structural  
575 biomass could potentially be investigated with this framework. However, additional  
576 measurements of storage and turnover would be highly beneficial for the performance of the  
577 simulation. Repeated observations over time are also useful, particularly for young plants, to  
578 account for variations in parameter values over time. We found significant changes in  
579 parameter values during the course of the 4-month experiment, which may be linked to both  
580 ontogeny and seasonal variation in temperature.

581 One major caveat on our results is that below-ground carbon cycling processes were not well  
582 characterized. For practical reasons, processes such as root growth, respiration, turnover, and  
583 exudation are rarely well quantified in empirical studies. Here, we had access to initial and  
584 final estimates of root biomass. Root respiration was estimated; root turnover and exudation  
585 were assumed to be zero. There is evidence that stress can increase rates of root exudation:  
586 for example, Karst et al. (2016) demonstrate increased exudation rates in seedlings exposed  
587 to cold soils. They also showed that stressed plants may exude C beyond that predicted by  
588 simple concentration gradients in NSC between root and soil. The loss of C independent of  
589 NSC in roots suggests that exudation may be actively enhanced once plant growth is limited  
590 (Hamilton et al., 2008; Karst et al., 2017). As our CBM does not include this process, it  
591 would attribute any C loss through root exudation to another process removing C from the  
592 plant, such as growth respiration. The increase in growth respiration that we inferred may



593 thus potentially include root exudation. Direct measurements of one or both processes would  
594 be required to determine the role of root exudation.

#### 595 **4.3 Implications for modelling plant growth under sink limited conditions**

596 The goal of our study was to examine how carbon balance models should be modified to  
597 represent sink limitation of growth, whilst maintaining mass balance. Our results demonstrate  
598 that several process representations need to be modified. Firstly, we demonstrate a clear need  
599 to incorporate a carbohydrate storage pool, with a dynamic utilization rate for growth. We  
600 demonstrate that the utilization rate is slowed by sink limitation, and may also vary with  
601 ontogeny. Targeted experimental work is needed to better quantify this variation in utilization  
602 rates. Secondly, in addition to a feedback on photosynthetic rates, other plant processes  
603 including growth respiration, turnover and allocation are also affected by sink limitation.  
604 Applying a DA-modelling framework to experimental data with rooting volume restriction  
605 has allowed us to quantify these effects in this experiment. Applying this approach more  
606 broadly would potentially allow us to identify general patterns in these responses that could  
607 then be formulated for inclusion into models. Overall, this approach provides important  
608 insights into the regulation of carbohydrate storage, and would significantly advance our  
609 ability to predict the impacts of environmental changes on plant growth and vulnerability to  
610 stress.

611

#### 612 **Data availability**

613 The raw data are freely available on Figshare (doi:  
614 <https://doi.org/10.6084/m9.figshare.5125087.v3>). The R source code to perform all the data  
615 processing and analysis to replicate the figures is freely available as a Git repository  
616 ([https://github.com/kashifmahmud/DA\\_Sink\\_limited\\_experiment](https://github.com/kashifmahmud/DA_Sink_limited_experiment)).

617

#### 618 **Author contribution**

619 KM analyzed the data, developed the model code, performed the simulations and wrote the  
620 paper. BEM conceived the idea and helped in data analysis. RAD and CC provided the  
621 experimental data. BEM, RAD, CC and MGD provided in-depth editing of the manuscript.

622

#### 623 **Competing interests**

624 The authors declare that they have no conflict of interest.

625



## 626 Acknowledgements

627 This research was supported by the Australian Research Council (Discovery, DP  
 628 DP160103436), the Hawkesbury Institute for the Environment, and Western Sydney  
 629 University. The authors wish to thank Burhan Amiji for his technical assistance and all  
 630 individuals from Hawkesbury Institute for the Environment who helped during the  
 631 experimental harvest. We thank Mathew Williams for advice on implementing the data  
 632 assimilation framework.

633

## 634 References

635 Arp, W. J.: Effects of source sink relations on photosynthetic acclimation to elevated carbon  
 636 dioxide, *Plant, Cell and Environment*, 14, 869-876, 1991.

637 Bloom, A. A., Exbrayat, J.-F., van der Velde, I. R., Feng, L., and Williams, M.: The decadal  
 638 state of the terrestrial carbon cycle: Global retrievals of terrestrial carbon allocation, pools,  
 639 and residence times, *Proceedings of the National Academy of Sciences*, 113, 1285-1290,  
 640 10.1073/pnas.1515160113, 2016.

641 BoM: Climate Data Online (Station 067105), Bureau of Meteorology Melbourne.  
 642 <http://www.bom.gov.au/climate/data/> (Accessed 26-08-2017). 2017.

643 Bossel, H.: treedyn3 forest simulation model, *Ecol. Model.*, 90, 187-227,  
 644 [https://doi.org/10.1016/0304-3800\(95\)00139-5](https://doi.org/10.1016/0304-3800(95)00139-5), 1996.

645 Bradford, K. J., and Hsiao, T. C.: Stomatal behavior and water relations of waterlogged  
 646 tomato plants, *Plant Physiol*, 70, 1508-1513, 1982.

647 Buckley, T. N.: The control of stomata by water balance, *New Phytologist*, 168, 275-292,  
 648 10.1111/j.1469-8137.2005.01543.x, 2005.

649 Campany, C. E., Medlyn, B. E., and Duursma, R. A.: Reduced growth due to belowground  
 650 sink limitation is not fully explained by reduced photosynthesis, *Tree Physiol*, 37, 1042-1054,  
 651 10.1093/treephys/tpx038, 2017.



- 652 Crous, K. Y., and Ellsworth, D. S.: Canopy position affects photosynthetic adjustments to  
653 long-term elevated CO<sub>2</sub> concentration (FACE) in aging needles in a mature *Pinus taeda*  
654 forest, *Tree Physiol*, 24, 961-970, 2004.
- 655 De Kauwe, M. G., Medlyn, B. E., Zaehle, S., Walker, A. P., Dietze, M. C., Wang, Y. P., Luo,  
656 Y. Q., Jain, A. K., El-Masri, B., Hickler, T., Warlind, D., Weng, E. S., Parton, W. J.,  
657 Thornton, P. E., Wang, S. S., Prentice, I. C., Asao, S., Smith, B., McCarthy, H. R., Iversen,  
658 C. M., Hanson, P. J., Warren, J. M., Oren, R., and Norby, R. J.: Where does the carbon go? A  
659 model-data intercomparison of vegetation carbon allocation and turnover processes at two  
660 temperate forest free-air CO<sub>2</sub> enrichment sites, *New Phytologist*, 203, 883-899,  
661 10.1111/nph.12847, 2014.
- 662 de Wit, C. T.: Simulation of assimilation, respiration, and transpiration of crops, Wiley, 1978.
- 663 de Wit, C. T., and van Keulen, H.: Modelling production of field crops and its requirements,  
664 *Geoderma*, 40, 253-265, [https://doi.org/10.1016/0016-7061\(87\)90036-X](https://doi.org/10.1016/0016-7061(87)90036-X), 1987.
- 665 Duan, H., Amthor, J. S., Duursma, R. A., O'Grady, A. P., Choat, B., and Tissue, D. T.:  
666 Carbon dynamics of eucalypt seedlings exposed to progressive drought in elevated [CO<sub>2</sub>] and  
667 elevated temperature, *Tree Physiol.*, 33, 779-792, 10.1093/treephys/tpt061, 2013.
- 668 Duursma, R. A.: YplantQMC: plant architectural analysis with Yplant and  
669 QuasiMC, 2014.
- 670 Duursma, R. A.: Plantecophys - An R Package for Analysing and Modelling Leaf Gas  
671 Exchange Data, *PLOS ONE*, 10, e0143346, 10.1371/journal.pone.0143346, 2015.
- 672 Farquhar, G. D., Von Caemmerer, S., and Berry, J. A.: A biochemical model of  
673 photosynthetic carbon dioxide assimilation in leaves of 3-carbon pathway species, *Planta*,  
674 149, 78-90, 1980.
- 675 Fatichi, S., Ivanov, V. Y., and Caporali, E.: Assessment of a stochastic downscaling  
676 methodology in generating an ensemble of hourly future climate time series, *Climate*  
677 *Dynamics*, 40, 1841-1861, 10.1007/s00382-012-1627-2, 2013.



- 678 Fatichi, S., Leuzinger, S., and Körner, C.: Moving beyond photosynthesis: from carbon  
679 source to sink-driven vegetation modeling, *New Phytologist*, 201, 1086-1095,  
680 10.1111/nph.12614, 2014.
- 681 Friend, A. D., Lucht, W., Rademacher, T. T., Keribin, R., Betts, R., Cadule, P., Ciais, P.,  
682 Clark, D. B., Dankers, R., Falloon, P. D., Ito, A., Kahana, R., Kleidon, A., Lomas, M. R.,  
683 Nishina, K., Ostberg, S., Pavlick, R., Peylin, P., Schaphoff, S., Vuichard, N., Warszawski, L.,  
684 Wiltshire, A., and Woodward, F. I.: Carbon residence time dominates uncertainty in  
685 terrestrial vegetation responses to future climate and atmospheric CO<sub>2</sub>, *Proceedings of the*  
686 *National Academy of Sciences*, 111, 3280-3285, 10.1073/pnas.1222477110, 2014.
- 687 Gunderson, C. A., and Wullschleger, S. D.: Photosynthetic acclimation in trees to rising  
688 atmospheric CO<sub>2</sub>: a broader perspective, *Photosynthesis Research*, 39, 369-388, 1994.
- 689 Hamilton, E. W., Frank, D. A., Hinchey, P. M., and Murray, T. R.: Defoliation induces root  
690 exudation and triggers positive rhizospheric feedbacks in a temperate grassland, *Soil Biology*  
691 *and Biochemistry*, 40, 2865-2873, <https://doi.org/10.1016/j.soilbio.2008.08.007>, 2008.
- 692 Hess, L., and De Kroon, H.: Effects of rooting volume and nutrient availability as an  
693 alternative explanation for root self/non-self discrimination, *J. Ecol.*, 95, 241-251,  
694 10.1111/j.1365-2745.2006.01204.x, 2007.
- 695 Hughes, I. G., and Hase, T. P. A.: *Measurements and their Uncertainties A Practical Guide to*  
696 *Modern Error Analysis*, Oxford University Press, Oxford, UK, 2010.
- 697 Jain, A. K., and Yang, X.: Modeling the effects of two different land cover change data sets  
698 on the carbon stocks of plants and soils in concert with CO<sub>2</sub> and climate change, *Global*  
699 *Biogeochemical Cycles*, 19, n/a-n/a, 10.1029/2004GB002349, 2005.
- 700 Karst, J., Gaster, J., Wiley, E., and Landhäusser, S. M.: Stress differentially causes roots of  
701 tree seedlings to exude carbon, *Tree Physiol.*, 37, 154-164, 10.1093/treephys/tpw090, 2017.
- 702 Körner, M., Waser, B., Rehmann, R., and Reubi, J. C.: Early over-expression of GRP  
703 receptors in prostatic carcinogenesis, *The Prostate*, 74, 217-224, 10.1002/pros.22743, 2014.



- 704 Law, R. M., Kowalczyk, E. A., and Wang, Y. P.: Using atmospheric CO<sub>2</sub> data to assess a  
705 simplified carbon-climate simulation for the 20th century, *Tellus Ser. B-Chem. Phys.*  
706 *Meteorol.*, 58, 427-437, 2006.
- 707 Maina, G. G., Brown, J. S., and Gersani, M.: Intra-plant versus inter-plant root competition in  
708 beans: avoidance, resource matching or tragedy of the commons, *Plant Ecology*, 160, 235-  
709 247, 2002.
- 710 McConnaughay, K. D. M., and Bazzaz, F. A.: Is Physical Space a Soil Resource?, *Ecology*,  
711 72, 94-103, 10.2307/1938905, 1991.
- 712 McMurtrie, R., and Wolf, L.: A model of competition between trees and grass for radiation,  
713 water and nutrients, *Annals of Botany (London)*, 52, 449-458, 1983.
- 714 Medlyn, B. E., Duursma, R. A., Eamus, D., Ellsworth, D. S., Prentice, I. C., Barton, C. V. M.,  
715 Crous, K. Y., de Angelis, P., Freeman, M., and Wingate, L.: Reconciling the optimal and  
716 empirical approaches to modelling stomatal conductance, *Glob. Change Biol.*, 17, 2134-2144,  
717 10.1111/j.1365-2486.2010.02375.x, 2011.
- 718 Metropolis, N., Rosenbluth, A. W., Rosenbluth, M. N., Teller, A. H., and Teller, E.: Equation  
719 of State Calculations by Fast Computing Machines, *J. Chem. Phys.*, 21, 10.1063/1.1699114,  
720 1953.
- 721 Mitchell, R. J., Liu, Y., O'Brien, J. J., Elliott, K. J., Starr, G., Miniati, C. F., and Hiers, J. K.:  
722 Future climate and fire interactions in the southeastern region of the United States, *Forest*  
723 *Ecology and Management*, 327, 316-326, <https://doi.org/10.1016/j.foreco.2013.12.003>, 2014.
- 724 Müller, C., Cramer, W., Hare, W. L., and Lotze-Campen, H.: Climate change risks for  
725 African agriculture, *Proceedings of the National Academy of Sciences*, 108, 4313-4315,  
726 10.1073/pnas.1015078108, 2011.
- 727 NeSmith, D. S., and Duval, J. R.: The Effect of Container Size, *HortTechnology*, 8, 495-498,  
728 1998.



- 729 Nikinmaa, E., Sievänen, R., and Hölttä, T.: Dynamics of leaf gas exchange, xylem and  
730 phloem transport, water potential and carbohydrate concentration in a realistic 3-D model tree  
731 crown, *Annals of Botany*, 114, 653-666, 10.1093/aob/mcu068, 2014.
- 732 Poorter, H., Böhler, J., van Dusschoten, D., Climent, J., and Postma, J. A.: Pot size matters: a  
733 meta-analysis of the effects of rooting volume on plant growth, *Funct Plant Biol*, 39, 839-  
734 850, 10.1071/fp12049, 2012a.
- 735 Poorter, H., Niklas, K. J., Reich, P. B., Oleksyn, J., Poot, P., and Mommer, L.: Biomass  
736 allocation to leaves, stems and roots: meta-analyses of interspecific variation and  
737 environmental control, *New Phytologist*, 193, 30-50, 10.1111/j.1469-8137.2011.03952.x,  
738 2012b.
- 739 Pugh, T. A. M., Müller, C., Arneth, A., Haverd, V., and Smith, B.: Key knowledge and data  
740 gaps in modelling the influence of CO<sub>2</sub> concentration on the terrestrial carbon sink, *Journal*  
741 *of Plant Physiology*, 203, 3-15, <https://doi.org/10.1016/j.jplph.2016.05.001>, 2016.
- 742 Reich, P. B.: Key canopy traits drive forest productivity, *Proceedings of the Royal Society B:*  
743 *Biological Sciences*, 10.1098/rspb.2011.2270, 2012.
- 744 Richardson, A. D., Williams, M., Hollinger, D. Y., Moore, D. J. P., Dail, D. B., Davidson, E.  
745 A., Scott, N. A., Evans, R. S., Hughes, H., Lee, J. T., Rodrigues, C., and Savage, K.:  
746 Estimating parameters of a forest ecosystem C model with measurements of stocks and fluxes  
747 as joint constraints, *Oecol.*, 164, 25-40, 10.1007/s00442-010-1628-y, 2010.
- 748 Richardson, A. D., Carbone, M. S., Keenan, T. F., Czimczik, C. I., Hollinger, D. Y.,  
749 Murakami, P., Schaberg, P. G., and Xu, X. M.: Seasonal dynamics and age of stemwood  
750 nonstructural carbohydrates in temperate forest trees, *New Phytologist*, 197, 850-861,  
751 10.1111/nph.12042, 2013.
- 752 Robbins, N. S., and Pharr, D. M.: Effect of Restricted Root Growth on Carbohydrate  
753 Metabolism and Whole Plant Growth of *Cucumis sativus* L, *Plant Physiol.*, 87,  
754 409-413, 10.1104/pp.87.2.409, 1988.





- 755 Rowland, L., Hill, T. C., Stahl, C., Siebicke, L., Burban, B., Zaragoza-Castells, J., Ponton, S.,  
756 Bonal, D., Meir, P., and Williams, M.: Evidence for strong seasonality in the carbon storage  
757 and carbon use efficiency of an Amazonian forest, *Glob. Change Biol.*, 20, 979-991,  
758 10.1111/gcb.12375, 2014.
- 759 Running, S. W., and Gower, S. T.: FOREST-BGC, A general model of forest ecosystem  
760 processes for regional applications. II. Dynamic carbon allocation and nitrogen budgets1,  
761 *Tree Physiol.*, 9, 147-160, 10.1093/treephys/9.1-2.147, 1991.
- 762 Sage, R. F.: Acclimation of photosynthesis to increasing atmospheric CO<sub>2</sub>: the gas-exchange  
763 perspective, *Photosynthesis Research*, 39, 351-368, 1994.
- 764 Sala, A., Woodruff, D. R., and Meinzer, F. C.: Carbon dynamics in trees: feast or famine?,  
765 *Tree Physiol.*, 32, 764-775, 10.1093/treephys/tpr143, 2012.
- 766 Schiestl-Aalto, P., Kulmala, L., Mäkinen, H., Nikinmaa, E., and Mäkelä, A.: CASSIA – a  
767 dynamic model for predicting intra-annual sink demand and interannual growth variation in  
768 Scots pine, *New Phytologist*, 206, 647-659, 10.1111/nph.13275, 2015.
- 769 Schwarz, G.: Estimating the Dimension of a Model, *Ann. Statist.*, 6, 461-464,  
770 10.1214/aos/1176344136, 1978.
- 771 Thornley, J. H. M., and Cannell, M. G. R.: Modelling the Components of Plant Respiration:  
772 Representation and Realism, *Annals of Botany*, 85, 55-67, 10.1006/anbo.1999.0997, 2000.
- 773 Thornton, P. E., Lamarque, J.-F., Rosenbloom, N. A., and Mahowald, N. M.: Influence of  
774 carbon-nitrogen cycle coupling on land model response to CO<sub>2</sub> fertilization and climate  
775 variability, *Global Biogeochemical Cycles*, 21, n/a-n/a, 10.1029/2006GB002868, 2007.
- 776 Van Oijen, M.: Bayesian Calibration (BC) and Bayesian Model Comparison (BMC) of  
777 Process-Based Models: Theory, Implementation and Guidelines, 2008.
- 778 Villar, R., and Merino, J.: Comparison of leaf construction costs in woody species with  
779 differing leaf life-spans in contrasting ecosystems, *New Phytologist*, 151, 213-226,  
780 10.1046/j.1469-8137.2001.00147.x, 2001.



- 781 Wiley, E., and Helliker, B.: A re-evaluation of carbon storage in trees lends greater support  
782 for carbon limitation to growth, *New Phytologist*, 195, 285-289, 10.1111/j.1469-  
783 8137.2012.04180.x, 2012.
- 784 Williams, M., Schwarz, P. A., Law, B. E., Irvine, J., and Kurpius, M. R.: An improved  
785 analysis of forest carbon dynamics using data assimilation, *Glob. Change Biol.*, 11, 89-105,  
786 2005.
- 787 Zaehle, S., and Friend, A. D.: Carbon and nitrogen cycle dynamics in the O-CN land surface  
788 model: 1. Model description, site-scale evaluation, and sensitivity to parameter estimates,  
789 *Global Biogeochemical Cycles*, 24, n/a-n/a, 10.1029/2009GB003521, 2010.
- 790 Zobitz, J. M., Desai, A. R., Moore, D. J. P., and Chadwick, M. A.: A primer for data  
791 assimilation with ecological models using Markov Chain Monte Carlo (MCMC), *Oecol.*, 167,  
792 599, 10.1007/s00442-011-2107-9, 2011.
- 793